

# INFLECTION-POINT S GOLDSTINO INFLATION IN NO-SCALE SUPERGRAVITY

CONSTANTINOS PALLIS

Laboratory of Physics, Faculty of Engineering, Aristotle University of Thessaloniki, GR-541 24 Thessaloniki, GREECE

e-mail address: kpallis@gen.auth.gr

**ABSTRACT:** We propose a modification of no-scale supergravity models which incorporates sgoldstino stabilization and supersymmetry (SUSY) breaking with a tunable cosmological constant by introducing a Kähler potential which yields a kinetic pole of order one. The resulting scalar potential may develop an inflection point, close to which an inflationary period can be realized for subplanckian field values consistently with the observational data. For central value of the spectral index  $n_s$ , the necessary tuning is of the order of  $10^{-6}$ , the tensor-to-scalar ratio  $r$  is tiny whereas the running of  $n_s$ ,  $a_s$ , is around  $-3 \cdot 10^{-3}$ . Our proposal is compatible with high-scale SUSY and the results of LHC on the Higgs boson mass.

PACs numbers: 12.60.Jv, 04.65.+e

Published in *Phys. Lett. B* **843**, 138018 (2023)

## I. INTRODUCTION

One of the most tantalizingly evasive problems in Particle Physics is the explanation of the large hierarchies existing in the fundamental scales of the modern theories. Two of these scales are related to the cosmological problems of inflation and *Dark Energy* (DE) whereas a third one is related to the scale of *Supersymmetry* (SUSY) breaking. The first of the scales above, is expected to be less than  $10^4$  EeV, the second one is related to the present acceleration of the Universe and is really very tiny ( $\Lambda \sim 1$  meV) whereas the scale of the SUSY partners,  $\tilde{m}$ , is continuously pushed more and more beyond the TeV region due to the lack of any positive signal at LHC until now.

In a set of recent papers [1, 2], two of the aforementioned scales ( $\tilde{m}$  and  $\Lambda$ ) are systematically interconnected within the framework of no-scale *Supergravity* (SUGRA) [3, 4]. Adopting simple Kähler potentials parameterizing flat or curved (compact or non-compact) Kähler manifolds, one can initially derive superpotentials which yield SUSY breaking along Minkowski flat directions. Combining two types of these superpotentials, *de Sitter* (dS) vacua are achieved which may, in addition, explain the notorious DE problem finely tuning a single superpotential parameter. In other words, these models offer a *technically natural* resolution to the DE problem. The construction can be easily extended to multi-modular settings of mixed geometry. Mild deformations of the adopted moduli geometry can cure possible instabilities and/or massless excitations. *Soft SUSY-Breaking* (SSB) parameters of the order of the gravitino ( $\tilde{G}$ ) mass  $m_{3/2}$  can be also derived. It is worth mentioning that the method above does not require any external mechanism for vacuum uplifting – see, e.g., Ref. [8, 9].

It would be certainly beneficial if we could incorporate in the aforementioned framework observationally acceptable inflation as done in Ref. [5, 6]. There the SUSY breaking sector is supplemented with the inflationary one which assures Starobinsky-like inflation consistently with data – for similar attempts see Ref. [11–15]. In contrast to those models, though, we here adopt the most economical possible interface of both sectors postulating that the scalar component of the goldstino superfield, – which is responsible for the SUSY breaking – plays the role of the inflaton – cf. Ref. [16–20]. Such a construction predicts directly the scale  $\tilde{m}$ , since the fundamental mass parameter,  $m$ , entering the superpotential

of goldstino is relied on the normalization [7] of the power spectrum of the curvature perturbation – cf. Ref. [18–20]. As a consequence,  $m_{3/2}$  and  $\tilde{m}$  lie at the EeV mass scale. Therefore, the set-up of high-scale SUSY [31, 32] naturally arises, as can be demonstrated by coupling the goldstino sector to the *Minimal SUSY Standard Model* (MSSM) [33] and deriving the relevant SSB parameters [34]. It is worth mentioning that these  $\tilde{m}$  values are compatible with the Higgs boson mass discovered at LHC [10] stabilizing, thereby, the electroweak vacuum.

To implement the inflationary scenario above we adopt a Kähler potential which generates a kinetic pole of order one [21] in the SUGRA lagrangian. The presence of this pole essentially restricts the dynamics of all the ingredients of our set-up (inflation, SUSY breaking and DE) to field values below the Planck scale. For specific values of the parameters the SUGRA potential develops an inflection point [20, 23–27] which supports inflationary solutions at the cost of a tuning of the order of  $10^{-6}$  in the selection of a relevant parameter. The realized *Inflection-Point inflation* (IPI) is a typical inflationary model – see, e.g., Ref. [22] – which was first introduced in the context of MSSM [23, 24] and then employed in various frameworks [20, 25–27]. To our knowledge, none of them combines IPI with the aforementioned merits of no-scale SUGRA. IPI discussed here occurs for subplanckian field values and is consistent with data [28, 29] predicting negligible production of primordial gravitational waves and testable [30] running of  $n_s$ . After its end, the universe is reheated up to a temperature [35] of PeV level via the perturbative decay of the heavy sgoldstino into gravitinos and/or MSSM (s)particles [36–39] via SUGRA-based interactions.

We start our presentation implementing the transition from Minkowski to dS vacua in the framework of our model in Sec. II. Then, in Sec. III, we verify the generation of the DE potential energy at the stable dS vacuum and, in Sec. IV, we extract the SSB terms. In Sec. V we focus on the exploration of the inflationary stage and, finally, we summarize our results in Sec. VI. Unless otherwise stated, we use units where the reduced Planck scale  $m_P = 2.4 \cdot 10^{18}$  GeV is taken to be unity, a subscript of type  $\chi$  denotes derivation *with respect to* (w.r.t.) the field  $\chi$  and charge conjugation is denoted by a star. We also recall that  $1 \text{ PeV} = 10^6 \text{ GeV}$  and  $1 \text{ EeV} = 10^9 \text{ GeV}$ .

arXiv:2302.12214v3 [hep-ph] 10 Aug 2023

## II. MODEL SET-UP

We work in the context of SUGRA employing just one chiral superfield  $Z$  – cf. Ref. [14, 16, 20]. The F-term SUGRA potential is given by

$$V = e^G \left( G^{ZZ^*} G_Z G_{Z^*} - 3 \right), \quad (1)$$

where  $G$  is the Kähler -invariant function defined in terms of the Kähler potential  $K = K(Z, Z^*)$  and the superpotential  $W = W(Z)$  as follows

$$G := K + \ln |W|^2 \text{ with } G_{ZZ^*} = K_{ZZ^*} = K_{,ZZ^*} \quad (2)$$

denoting the Kähler metric and  $G^{ZZ^*}$  is its inverse. We concentrate on the following  $K$

$$K = -N \ln \Omega \text{ with } \Omega = 1 - (Z + Z^*)/2 + k^2 Z_v^4, \quad (3a)$$

where  $N > 0$  and we include in the argument of  $\ln$  the stabilization term

$$Z_v = Z + Z^* - 2v. \quad (3b)$$

Here  $k$  and  $v$  are two real free parameters. The  $Z$  space generated by  $K$  for  $k = 0$  is hyperbolic and invariant under a set of transformations related to the group  $U(1, 1)$  – see Ref. [21]. Small  $k$ 's are completely natural, according to the 't Hooft argument [40], thanks to the enhanced symmetry above.

Following our strategy in Ref. [1, 2] we first substitute  $K$  in Eq. (3a) with  $k = 0$  together with an unspecified  $W$  into Eq. (1) taking the limit  $Z = Z^*$  – the stability of this path is checked a posteriori below. We obtain

$$V = \omega^{-N} W^2 \left( \frac{4\omega^2}{N} \left( \frac{N}{2\omega} + \frac{dW}{dZW} \right)^2 - 3 \right), \quad (4)$$

where we introduce the shorthand notation

$$\omega = \Omega(Z = Z^*, k = 0) = 1 - Z. \quad (5)$$

A  $Z$ -flat direction with Minkowski vacua can be assured if we seek  $W = W_0$  such that  $V = 0$  for any  $Z$ .  $W_0$  can be determined solving the resulting ordinary differential equation

$$\frac{dW_0}{W_0} = n_{\pm} \frac{dZ}{\omega} \text{ with } n_{\pm} = \frac{1}{2} \left( N \pm \sqrt{3N} \right). \quad (6)$$

For  $N = 3$  we obtain  $n_{\pm} = 0$  and we reveal the archetypal no-scale model [3] which exclusively yields Minkowski vacua. For  $N \neq 3$ , we obtain two possible forms of  $W_0$ ,

$$W_0^{(\pm)}(Z) = m\omega^{n_{\pm}}, \quad (7)$$

where  $m$  is an arbitrary mass parameter which agrees with the one introduced for the Polónyi model [4]. The exponents  $n_{\pm} \neq 0$  may, in principle, acquire any real value, if we consider  $W_0$  as an effective superpotential including perturbative and non-perturbative contributions from string theory

[1]. However, when  $N/3$  is a perfect square, integer  $n_{\pm}$  values may arise too. E.g., for  $N = 12, 27$  and  $48$  we obtain  $(n_-, n_+) = (3, 9), (9, 18)$  and  $(18, 30)$  respectively.

The solutions in Eq. (7) can be combined as follows

$$W_{\Lambda} = W_0^{(+)} - C_{\Lambda} W_0^{(-)} = m\omega^{n_+} C_{\omega}^{-}, \quad (8)$$

where we normalize somehow the relevant coefficients – cf. Ref. [2] – setting that multiplying  $W_0^{(+)}$  equal to unity. Also,

$$C_{\omega}^{\pm} := 1 \pm C_{\Lambda} \omega^{-\sqrt{3N}} \quad (9)$$

and reduces to unity for tiny  $C_{\Lambda}$  – see below. The resulting potential,  $V = V_{\Lambda}$ , obtained after replacing Eqs. (3a) and (8) into Eq. (1), is

$$V_{\Lambda} = m^2 \Omega^{-N} \omega^{2n_+} \left( |U/2\omega|^2 - 3|C_{\omega}^{-}|^2 \right), \quad (10)$$

where we define the quantity

$$U = \frac{\sqrt{2N}}{J\Omega} \left( \left( \sqrt{3}C_{\omega}^{+} + \sqrt{N}C_{\omega}^{-} \right) \Omega + 2\sqrt{N}C_{\omega}^{-} \Omega_{,Z\omega} \right). \quad (11)$$

Here  $J$  is related to the canonical normalization of the complex scalar field  $Z = ze^{i\theta}$  according to which

$$d\hat{z}/dz = \sqrt{2K_{ZZ^*}} = J \text{ and } \hat{\theta} = J\theta z, \quad (12)$$

where  $J$  can be expressed in terms of  $\Omega$  as follows

$$J = \sqrt{2N} \left( \frac{\Omega_{,Z}^2}{\Omega^2} - \frac{\Omega_{,ZZ^*}}{\Omega} \right)^{1/2}. \quad (13)$$

The involved derivatives of  $\Omega$  are found to be

$$\Omega_{,Z} = -1/2 + 4k^2 Z_v^3 \text{ and } \Omega_{,ZZ^*} = 12k^2 Z_v^2. \quad (14)$$

The structure of  $V_{\Lambda}$  in Eq. (10) is shown in Fig. 1 where the dimensionless quantity  $10^2 V_{\Lambda}/m^2 m_{\text{p}}^2$  is plotted as a function of  $z$  and  $\theta$  for the  $N, v, k, m$  and  $C_{\Lambda}$  values shown in Table I – we select the lower  $N$  which yields integer  $n_{\pm} > 0$ . We see that  $V_{\Lambda}$  develops along the stable direction  $\theta = 0$  (i) A dS vacuum for  $z = v = 0.5$  which interprets DE – see Sec. III – and breaks SUSY – see Sec. IV –, and (ii) an inflection point for  $z = z_0 \simeq 0.71$ , suitable for driving IPI – see Sec. V. The last finding seems to be a consequence of the adopted  $\Omega$  in Eq. (3a), since replacing its  $k$ -independent part with  $Z + Z^*$  or  $1 - |Z|^2$  and repeating the procedure above, the resulting  $V_{\Lambda}$  does not possess inflection point but it acquires a shape resembling that presented in Ref. [18, 19].

## III. DARK ENERGY

The stability of  $V_{\Lambda}$  at its dS – for  $C_{\Lambda} > 0$  – vacuum noticed by Fig. 1 can be analytically verified in general. Namely, we can show that the vacuum

$$\langle z \rangle = v \text{ and } \langle \theta \rangle = 0 \text{ with } \langle V_{\Lambda} \rangle = 12C_{\Lambda} m^2 \quad (15)$$

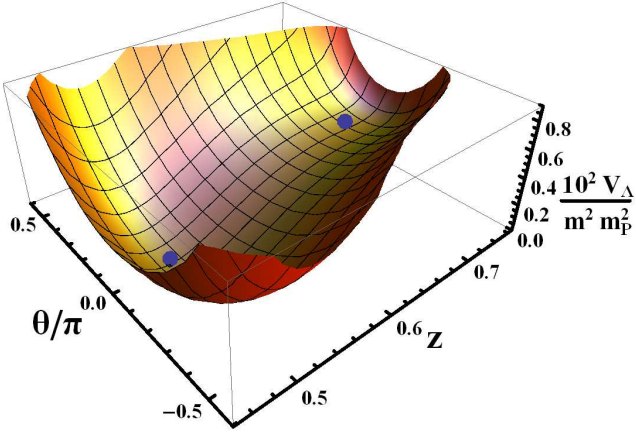


**FIG. 1:** The (dimensionless) SUGRA potential  $10^2 V_\Lambda / m^2 m_P^2$  in Eq. (10) as a function of  $z$  and  $\theta$  defined above Eq. (12) for the inputs shown in Table I. The location of the dS vacuum at  $(\langle z \rangle, \theta) = (0.5, 0)$  and the inflection point at  $(z_0, \theta) \simeq (0.71, 0)$  is also depicted by two thick points.

is stable against fluctuations of the various excitations for  $N > 3$ . In fact, the resulting masses squared of the canonically normalized scalars are found to be

$$m_z = 48m_{3/2}kN^{-1/2} \left\langle \omega^{3/2} C_\omega^+ / C_\omega^- \right\rangle; \quad (16a)$$

$$m_\theta = 2m_{3/2} \left( 1 - (3/N) \left\langle C_\omega^+ / C_\omega^- \right\rangle^2 \right)^{1/2} \quad (16b)$$

and the  $N > 3$  assures  $m_\theta^2 > 0$ . The  $\tilde{G}$  mass contained in the expressions above can be determined as follows

$$m_{3/2} = \left\langle e^{G/2} \right\rangle = \left\langle m\omega^{\sqrt{3N}/2} C_\omega^- \right\rangle. \quad (17)$$

Since  $\omega < 1$  from Eq. (5) and  $\sqrt{3N}/2 > 1$ , we infer that  $m_{3/2} \leq m$  and so all the aforementioned masses share approximately the same size. This is also confirmed from the sample values accumulated in the third from the bottom row of Table I.

An interpretation of DE can be achieved by demanding

$$\langle V_\Lambda \rangle = \Omega_\Lambda \rho_{c0} = 7.2 \cdot 10^{-121} m_P^4, \quad (18)$$

where  $\Omega_\Lambda = 0.6889$  and  $\rho_{c0} = 2.4 \cdot 10^{-120} h^2 m_P^4$  with  $h = 0.6732$  [7] is the density parameter of DE and the current critical energy density of the universe. As shown in Table I, the required value of  $C_\Lambda$  signals a serious fine tuning whose the origin remains elusive within our proposal. However, this value does not influence the remaining sectors of the model and can be selected in the definition of  $W_\Lambda$ .

#### IV. SUSY BREAKING

The SUSY breaking occurred at the vacuum in Eq. (15) can be transmitted to the visible world if we specify a reference

**TABLE I:** Sample-Point Parameters With Units Reinstalled (Values in curly brackets are obtained by the analytic expressions)

MODEL PARAMETERS				
$m/m_P$	$C_\Lambda/10^{-108}$	$N$	$k/0.1$	$v/m_P$
$5.6 \cdot 10^{-7}$	2.5	12	4.0167291	0.5
$(n_+, n_-) = (9, 3)$				
INFLECTION POINT LOCALIZATION				
$k_0/0.1$	$z_0/0.1m_P$	$\delta k/10^{-6}$	$\delta z_*/10^{-4}m_P$	
4.0166971	7.07433	3.20232	-1.5 {-1.1}	
EXPANSION PARAMETERS				
$v_0/(mm_P)^2$	$v_1/(mm_P)^2$	$v_2/(mm_P)^2$	$v_3/(mm_P)^2$	$J_0$
$3.9 \cdot 10^{-3}$	$1.5 \cdot 10^{-6}$	$-2.1 \cdot 10^{-6}$	2.2	5.4
INFLATION RESULTS				
$n_s$	$r/10^{-8}$	$-a_s/10^{-3}$	$10^5 A_s^{1/2}$	$N_*$
0.966 {0.97}	4.8 {3.9}	3.3 {3.2}	4.59 {4.27}	46.5 {45}
$V_{I_*}^{1/4}/\text{EeV}$	$H_{I_*}/\text{EeV}$	$\delta z_f/10^{-2}m_P$		$m_{\theta I_*}/H_{I_*}$
$4.6 \cdot 10^5$	49.5	-1.16 {-0.87}		5.1
POST-INFLATION RESULTS				
$m_z/\text{EeV}$	$m_\theta/\text{EeV}$	$m_{3/2}/\text{EeV}$	$\Gamma_{3/2}/\text{keV}$	$T_{\text{rh}}/\text{PeV}$
319	281	162	85	4.9
$\hat{\mu}/\text{EeV}$	$\tilde{m}$	$ A /\text{EeV}$	$ B /\text{EeV}$	$ M_a /\text{EeV}$
81	162	1024	1200	81.1

low energy model. We here adopt MSSM and the total superpotential,  $W_{\Lambda O}$ , of the theory takes the form [34]

$$W_{\Lambda O} = W_\Lambda(Z) + W_{\text{MSSM}}(\Phi_\alpha), \quad (19)$$

where  $W_{\text{MSSM}}$  has the well-known form written in short as

$$W_{\text{MSSM}} = h_{\alpha\beta\gamma} \Phi_\alpha \Phi_\beta \Phi_\gamma / 6 + \mu H_u H_d \quad (20)$$

with the various chiral superfields encoded as

$$\Phi_\alpha = Q, L, d^c, u^c, e^c, H_d \text{ and } H_u,$$

and we suppress the generation indices. We also denote the three non-vanishing Yukawa coupling constants as  $h_{\alpha\beta\gamma} = h_D, h_U$  and  $h_E$  for  $(\alpha, \beta, \gamma) = (Q, H_d, d^c), (Q, H_u, u^c)$  and  $(L, H_d, e^c)$  respectively. As we see below, our model fits well with the high-scale SUSY [31, 32] and therefore  $\mu$  acquires values close to  $m_{3/2}$ . We here handle it as a free parameter. On the other hand, we consider two simple variants of the total  $K$  of the theory,  $K_{\Lambda O}$ , ensuring SSB parameters for  $\Phi_\alpha$ :

$$K_{1\Lambda O} = K(Z) + \sum_\alpha |\Phi_\alpha|^2; \quad (21a)$$

$$K_{2\Lambda O} = K(Z) + N_O \ln(1 + \sum_\alpha |\Phi_\alpha|^2 / N_O), \quad (21b)$$

where  $N_O$  may remain unspecified. Note that if we expand  $K_{2\Lambda O}$  for low  $\Phi_\alpha$  values, the result coincides with  $K_{1\Lambda O}$ .

Adapting the general formulae of Ref. [34], we find universal (i.e.,  $\tilde{m}_\alpha = \tilde{m}$  and  $A_{\alpha\beta\gamma} = A$ ) SSB terms in the effective low energy potential which can be written as

$$V_{\text{SSB}} = \tilde{m}^2 |\Phi_\alpha|^2 + \left( \frac{1}{6} A \hat{h}_{\alpha\beta\gamma} \Phi_\alpha \Phi_\beta \Phi_\gamma + B \hat{\mu} H_u H_d + \text{h.c.} \right) \quad (22)$$

where the normalized (hatted) parameters are defined as

$$\langle \hat{h}_{\alpha\beta\gamma}, \hat{\mu} \rangle = \langle \omega \rangle^{-N/2} (h_{\alpha\beta\gamma}, \mu), \quad (23)$$

whereas the SSB parameters are found to be

$$\tilde{m} = m_{3/2}, \quad |A| = \sqrt{3N}m_{3/2} \quad \text{and} \quad |B| = (1 + \sqrt{3N})m_{3/2}. \quad (24)$$

Values for these parameters are displayed in Table I for  $\hat{\mu} = m_{3/2}/2$ . We see that  $|A| > m_{3/2}$  and  $|B| > m_{3/2}$  due to large  $N$  adopted there. However, these parameters have very suppressed impact on the SUSY mass spectra.

Similar values for the gauginos of MSSM are also expected. E.g., we may select the gauge-kinetic function [34] as

$$f_a = \lambda_a Z \quad (25)$$

where  $\lambda_a$  is a free parameter absorbed by a redefinition of the relevant spinors and  $a = 1, 2, 3$  runs over the factors of the gauge group of MSSM,  $U(1)_Y$ ,  $SU(2)_L$  and  $SU(3)_c$  respectively. In a such case, we find [34]

$$|M_a| = \sqrt{3/N} \langle \omega/z \rangle m_{3/2}, \quad (26)$$

which is obviously of the order of  $m_{3/2}$  – see e.g. Table I.

Scenarios with large  $\tilde{m}$ , although not directly accessible at the LHC, can be probed via the measured value of the Higgs boson mass. Within high-scale SUSY, updated analysis requires [10, 32]

$$3 \lesssim \tilde{m}/\text{EeV} \lesssim 300, \quad (27)$$

for degenerate sparticle spectrum, low  $\tan\beta$  values and minimal stop mixing. From Eq. (24) and the values in Table I we conclude that our setting is comfortably compatible with the requirement above.

## V. INFLECTION-POINT INFLATION

We analyze here the inflationary sector of our model. In Sec. VA we outline our method for the determination of the inflection point of the potential and in Sec. VB we describe our semi-analytic approach to inflationary dynamics. Then, in Sec. VC, we discuss the reheat process and in Sec. VD the parameters of our model are confronted with observations.

### A. INFLECTION-POINT CONDITIONS

The inflationary potential  $V_I = V_I(z)$  is obtained from  $V_\Lambda(Z)$  in Eq. (10), setting  $\theta = 0$  and  $C_\Lambda \simeq 0$ . Let us initially clarify that  $V_I$  develops discontinuities due to the denominator of  $U$  in Eq. (11) or the numerator of  $J$  in Eq. (13). In view of Eq. (14), these singularities can be determined by solving numerically the equation

$$256k^4(z-v)^6 + 16k^2(z-v)^2(z+2v-3) + 1/4 = 0. \quad (28)$$

In Fig. 2 we represent the segments of  $V_I$  as a function of  $z$  which are continuously connected with the vacuum in

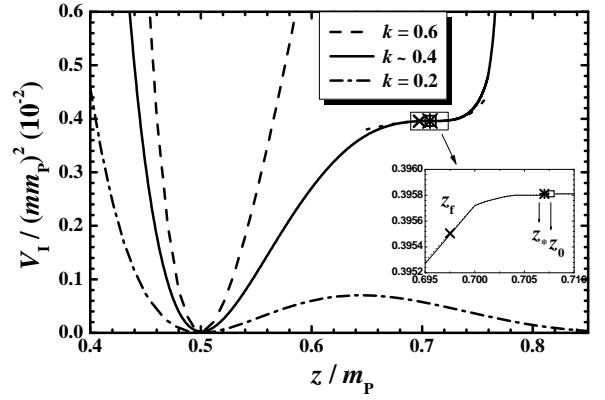


FIG. 2: Dimensionless inflationary potential  $V_I/m^2 m_p^2$  as a function of  $z$  for  $k = 0.40167291$  (black line) or  $k = 0.2$  (dot-dashed line) or  $k = 0.6$  (dashed line) and the remaining inputs in Table I. The dotted line is obtained by Eq. (33). The values of  $z_*$ ,  $z_f$  and  $z_0$  (for the first case) are also indicated.

Eq. (15). For the model parameters shown in Table I  $V_I$  exhibits poles at the points  $(z_{1p}, z_{2p}, z_{3p}) = (0.26, 0.78, 1.2)$  and is plotted by a solid line for  $z_{1p} \lesssim z \lesssim z_{2p}$ . Thanks to the interplay of the two opposing contributions in the parenthesis in Eq. (10), a step is generated for  $v < z < z_{2p}$ . The emergence of the inflationary plateau, though, crucially depends on  $k$ . Indeed, for  $k = 0.2$  and  $k = 0.6$  and keeping the residual inputs in Table I, we obtain the dot-dashed and dashed lines respectively in Fig. 2 where no inflection point is localized. We find  $(z_{1p}, z_{2p}) = (0.05, 1.21)$  in the former case and  $(z_{1p}, z_{2p}, z_{3p}) = (0.34, 0.68, 1.1)$  in the latter.

To localize the position of the inflection point, we impose

$$V_I'(z) = V_I''(z) = 0 \quad \text{for } v < z < 1, \quad (29)$$

where prime stands for derivation w.r.t  $z$ . These conditions can be translated as follows

$$\sqrt{3N}\Omega + N(\Omega + \omega\Omega') = 2\Omega U \frac{U + \omega U'}{U^2 - 12\omega^2}; \quad (30a)$$

$$N\Omega\omega \left( 4\Omega'(n_+ - 1)U^2 + \omega \left( 12\omega \left( \sqrt{3N} + N^2 \right) + 2UU' \right) \right) + \Omega^2 \left( U^2 N_1 + \omega \left( 4(1 - n_+)U^{2'} - \omega \left( 12N_2 - (U^2)'' \right) \right) \right) = (12\omega^2 - U^2) (\Omega''\omega + N(1 + N)\Omega'\omega^2), \quad (30b)$$

where we define the quantities

$$\begin{aligned} N_1 &= 6 - 5\sqrt{3N} - 2N + \sqrt{3N^3} + N^2; \\ N_2 &= 2N - \sqrt{3N} + 2\sqrt{3N^3} + N^2. \end{aligned} \quad (31)$$

Note that the conditions above are independent from the parameters  $m$  and  $C_\Lambda$  of  $W_\Lambda$ . Solving the conditions above w.r.t  $k$  and  $z$ , for every selected  $v$  and  $N$ , we can specify  $k = k_0$ , for which we obtain an inflection point, and its position at  $z = z_0$ . The output of this procedure is given in Fig. 3 where we plot  $(k_0, z_0)$  for  $N = 4, 10$  and  $30$  (dashed, solid and dot-dashed line respectively). Along each line we show the

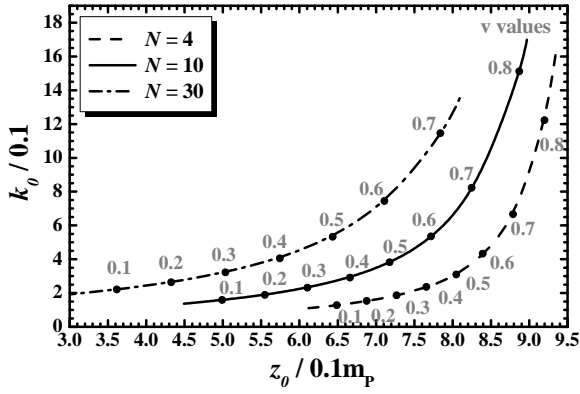


FIG. 3: Location of the inflection point in the  $z_0 - k_0$  plane for various  $N$ 's indicated in the plot. Shown is also the variation of  $v$  in grey along the lines.

variation of  $v$  in grey. We observe that the maximal allowed  $v$  values decrease as  $N$  increases whereas for  $v < 0.01$  the  $(k_0, z_0)$ 's remain almost constant. We also remark that  $z_0 > v$  and it remains subplanckian whereas the required  $k_0 < 1$  is quite natural, although it has to be determined using a precision up to six digits to be reliable.

### B. INFLATION ANALYSIS

Once we determine the  $(k_0, z_0)$  values, we can investigate the realization of IPI which is delimited by the condition [22]

$$\max\{\epsilon(\hat{z}), |\eta(\hat{z})|\} \leq 1, \quad (32a)$$

where the slow-roll parameters  $\epsilon$  and  $\eta$  read

$$\epsilon = \left( V_{I,\hat{z}} / \sqrt{2} V_I \right)^2 \quad \text{and} \quad \eta = V_{I,\hat{z}\hat{z}} / V_I \quad (32b)$$

and can be derived by employing  $V_I$  in Eq. (10) for  $\theta = 0$  and  $J$  in Eq. (13), without express explicitly  $V_I$  in terms of  $\hat{z}$ . Due to the complicate form of  $V_I$ , the analytic approach to the inflationary dynamics is not doable. Some progress can be made, if we use as input for our analytic treatment the numerical expansions of  $V_I$  and  $J$  about  $z = z_0$ ,

$$V_I \simeq v_0 + v_1 \delta z + v_2 \delta z^2 + v_3 \delta z^3 \quad \text{and} \quad J \simeq J_0, \quad (33)$$

where  $\delta z = z - z_0$ ,  $v_0 = V_I(z_0)$  and  $J_0 = J(z_0)$ . Since the observationally relevant part of IPI takes place quite close to  $z_0$ , the approximation above is quite accurate. This is confirmed in Fig. 2 where the dotted line, obtained by Eq. (33), is plotted against the exact result of  $V_I$  for the inputs in Table I. The relevant expansion coefficients are listed there. Thanks to the conditions in Eq. (29),  $v_1 = V_I'(z_0)$  and  $v_2 = V_I''(z_0)/2$  are quite suppressed compared to  $v_0$  and  $v_3$  and so we may neglect terms with  $v_1^2$ ,  $v_2^2$  and  $v_1 v_2$  below. Namely, inserting Eq. (33) into Eq. (32b) we arrive at the following results

$$\sqrt{\epsilon} \simeq \frac{v_1 + \delta z(2v_2 + 3\delta z v_3)}{\sqrt{2} J_0 v_0} \quad \text{and} \quad \eta \simeq \frac{2(v_2 + 3\delta z v_3)}{J_0^2 v_0}, \quad (34)$$

from which we can verify that Eq. (32a) is saturated for  $\delta z = \delta z_f$ , found from the condition

$$\eta(\delta z_f) \simeq 1 \Rightarrow \delta z_f \simeq -(J_0^2 v_0 + 2v_2)/6v_3. \quad (35)$$

Given that  $J_0^2 v_0 \gg v_2$ , we expect  $\delta z_f < 0$  or  $z_f < z_0$ .

The number of e-foldings  $N_*$  that the scale  $k_* = 0.05/\text{Mpc}$  experiences during IPI and the amplitude  $A_s$  of the power spectrum of the curvature perturbations generated by  $z$  can be computed using the standard formulae

$$N_* = \int_{\hat{z}_f}^{\hat{z}_*} d\hat{z} \frac{V_I}{V_{I,\hat{z}}} \quad \text{and} \quad A_s = \frac{1}{12\pi^2} \frac{V_I^3}{V_{I,\hat{z}}^2} \Big|_{\hat{z}=\hat{z}_*}, \quad (36)$$

where  $z_*$  [ $\hat{z}_*$ ] is the value of  $z$  [ $\hat{z}$ ] when  $k_*$  crosses the inflationary horizon. From the leftmost relation we find

$$N_* = (f_{N_*} - f_{N_f})/p_N \quad \text{where} \quad p_N = \sqrt{3v_1 v_3}/J_0^2 v_0 \quad (37)$$

and  $f_{N_*} = f_N(\delta z_*)$  and  $f_{N_f} = f_N(\delta z_f)$  with

$$f_N(z) = \arctan(v_2 + 3z v_3 / \sqrt{3v_1 v_3}). \quad (38)$$

Since  $\delta z_f$  turns out to be close to  $\delta z_*$  – as depicted in Fig. 2 – both contributions in Eq. (37) are important. Solving it w.r.t  $\delta z_*$  we obtain

$$\delta z_* \simeq -\frac{v_2}{3v_3} + \sqrt{\frac{v_1}{3v_3}} \tan\left(\frac{\sqrt{3}N_*}{J_0^2 v_0} + f_{N_f}\right), \quad (39)$$

from which we can deduce that  $z_* < z_0$  – see inset of Fig. 2. Plugging it into the rightmost equation in Eq. (36), we obtain

$$A_s^{1/2} \simeq \frac{J_0 v_0^{3/2}}{2\sqrt{3}\pi v_1} \cos^2(p_N N_* + f_{N_f}). \quad (40)$$

The remaining inflationary observables are found from

$$n_s = 1 - 6\epsilon_* + 2\eta_*, \quad r = 16\epsilon_*, \quad (41a)$$

$$a_s = 2(4\eta_*^2 - (n_s - 1)^2)/3 - 2\xi_*, \quad (41b)$$

where  $\xi = V_{I,\hat{z}} V_{I,\hat{z}\hat{z}\hat{z}} / V_I^2$  and the variables with subscript  $*$  are evaluated at  $z = z_*$ . Inserting  $\delta z_*$  from Eq. (39) into Eq. (32b) and then into equations above we obtain

$$n_s \simeq 1 + 4p_N \tan(p_N N_* + f_{N_f}), \quad (42a)$$

$$r \simeq 8v_1^2 \cos^{-4}(p_N N_* + f_{N_f}) / J_0^2 v_0^2, \quad (42b)$$

$$a_s \simeq -4p_N \cos^{-2}(p_N N_* + f_{N_f}). \quad (42c)$$

For the inputs of Table I, the results of our semianalytic approach are displayed in curly brackets and compared with those obtained using the pure numerical program. The proximity of both results is certainly impressive.

From Table I we may also infer that the semiclassical approximation, used in our analysis, is perfectly valid since  $V_{I_*}^{1/4} \ll m_{\text{P}}$ . Moreover, the  $\theta = 0$  direction is well stabilized and does not contribute to the curvature perturbation, since for the relevant effective mass  $m_{\theta I}$  we find  $m_{\theta I}^2 > 0$  for  $N > 3$  and  $m_{\theta I_*}/H_{I_*} > 1$  where  $H_I = (V_I/3)^{1/2}$ . We also checked that the one-loop radiative corrections,  $\Delta V_I$ , to  $V_I$  induced by  $m_{\theta I}$  let intact our inflationary outputs, provided that we take for the renormalization-group mass scale  $Q = m_{\theta I_*}$ . Since  $Q$  is close to  $V_{I_*}^{1/4}$  we do not expect sizable running of the quantities measured at  $Q$  – cf. Ref. [41].

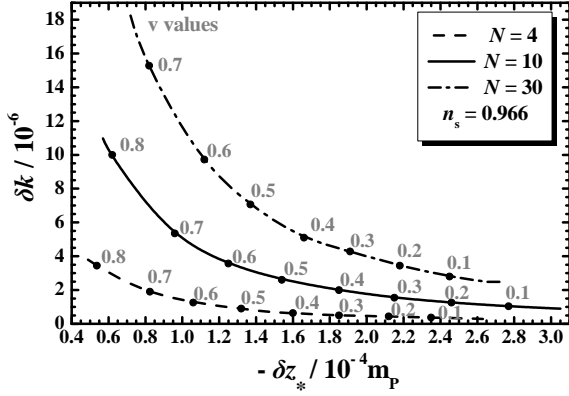


FIG. 4: Allowed curves in the  $(-\delta z_*) - \delta k$  plane for  $n_s \simeq 0.966$  and various  $N$ 's indicated in the plot. Shown is also the variation of  $v$  in grey along the lines.

### C. SGOLDSTINO DECAY

Soon after the end of IPI, the (canonically normalized) sgoldstino

$$\widehat{\delta z} = \langle J \rangle \delta z \text{ with } \delta z = z - v \text{ and } \langle J \rangle = \sqrt{\frac{N}{2}} \frac{1}{\langle \omega \rangle} \quad (43)$$

settles into a phase of damped oscillations around the minimum in Eq. (15) reheating the universe at a temperature [35]

$$T_{\text{rh}} = (72/5\pi^2 g_{\text{rh}*})^{1/4} \Gamma_{\delta z}^{1/2} m_{\text{P}}^{1/2}, \quad (44a)$$

where  $g_{\text{rh}*} = 106.75$  counts the effective number of the relativistic degrees of freedom at  $T_{\text{rh}}$ . The total decay width,  $\Gamma_{\delta z}$ , of  $\widehat{\delta z}$  predominantly includes the contributions

$$\Gamma_{\delta z} \simeq \Gamma_{3/2} + \Gamma_{\theta} + \Gamma_{\tilde{h}}, \quad (44b)$$

where the individual decay widths – which stem from SUGRA-induced interactions [36–39] – are found to be

$$(\Gamma_{3/2}, \Gamma_{\theta}, \Gamma_{\tilde{h}}) \simeq \left( \frac{\langle \omega \rangle^{-\sqrt{3N}} m_z^5}{96\pi m^2 m_{\text{P}}^2}, \frac{m_z^3}{16N\pi v m_{\text{P}}}, \frac{N\widehat{\mu}^2 m_z}{16\pi m_{\text{P}}^2} \right). \quad (45)$$

They express decay of  $\widehat{\delta z}$  into gravitinos, pseudo-sgoldstinos and higgsinos via the  $\mu$  term respectively. Thanks to the appearance of  $N$  in  $\Gamma_{\tilde{h}}$ , it is rather enhanced for large  $N$ 's.

### D. PARAMETER SPACE

In order to delineate the available parameter space of the model, we confront the quantities in Eq. (36) with the observational requirements [7]

$$N_* \simeq 61 + \ln(\pi v_0 T_{\text{rh}}^2)^{1/6} \text{ and } A_s \simeq 2.1052 \cdot 10^{-9}, \quad (46)$$

where we assume that IPI is followed in turn by an oscillatory phase, with mean equation-of-state parameter  $w_{\text{rh}} \simeq 0$ ,

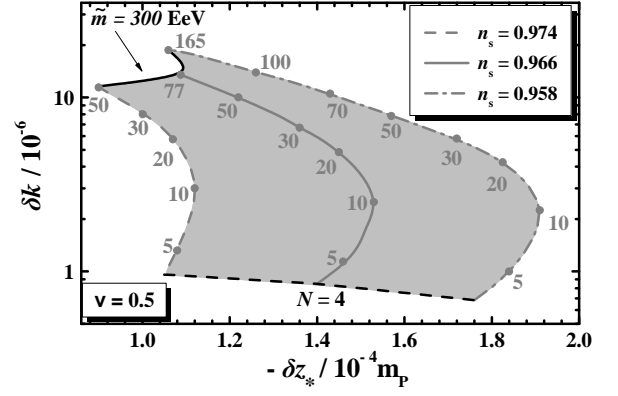


FIG. 5: Allowed (shaded) region in the  $(-\delta z_*) - \delta k$  plane for  $v = 0.5$ . The constraint fulfilled along each line and the variation of  $N$  are also shown in black and grey respectively.

radiation and matter domination. The remaining observables must be in agreement with the fitting of the *Planck* TT, TE, EE+lowE+lensing, BK15 (from BICEP2/Keck Array) [29] and BAO data [28] with the  $\Lambda\text{CDM}+r+a_s$  model which requires

$$n_s = 0.9658 \pm 0.008 \text{ and } a_s = -0.0066 \pm 0.014 \quad (47)$$

at 95% confidence level. Recall that the upper bound on  $r$  is irrelevant in our case since  $r$  is negligible – see Sec. VB.

In our numerical program for any selected  $N$  and  $v$  – see Eq. (10) – we compute  $(k_0, z_0)$  solving numerically Eq. (29). Then enforcing Eq. (46) we can restrict  $\delta k = k - k_0$  and  $m$  whereas the leftmost observable in Eq. (47) determines  $\delta z_*$ . From Eq. (41b) the model's predictions regarding  $a_s$  and  $r$  can be computed. Increasing  $\delta k$  allows us to increase the slope of the plateau around  $z_0$  decreasing, thereby,  $N_*$ . Note that the  $\delta k$  does not appear in the formulae in Sec. VB, since the relevant information is encoded in Eq. (33).

The outputs of our numerical investigation can be presented in the  $(-\delta z_*) - \delta k$  plane as in Figs. 4 and 5. In the first one we fix  $N$  to three representative values 4, 10 and 30 and display the allowed curves (dot-dashed, solid and dashed lines respectively) taking the central  $n_s$  value in Eq. (47). The variation of  $v$  along each line is displayed in grey. On the other hand, in Fig. 5 we set  $v = 0.5$  and identify the allowed (shaded) region allowing  $n_s$  to vary in the margin of Eq. (47). The variation of  $N$  is shown along each line. The allowed region is bounded by (i) the solid black line, which corresponds to the upper bound in Eq. (27), (ii) the dashed black line which originates from the lower bound on  $N$  derived in Sec. III and (iii) the dot-dashed and dashed gray lines along which the lower and upper bounds on  $n_s$  in Eq. (47) are saturated respectively. We remark that increasing  $|\delta z_*|$ , decreases  $n_s$  with fixed  $\delta k$ . From both figures we deduce that the achievement of observationally acceptable IPI requires a tuning of the order of  $10^{-6}$  which is somehow ameliorated as  $N$  increases. This tuning though is milder than that needed within the conventional MSSM [24].

Fixing  $n_s \simeq 0.966$ , we obtain the gray solid line in Fig. 5, along which we obtain the mass spectrum shown in Fig. 6 as a function of  $m$ . Namely, we depict  $m_{3/2}$ ,  $m_z$  and  $m_{\theta}$

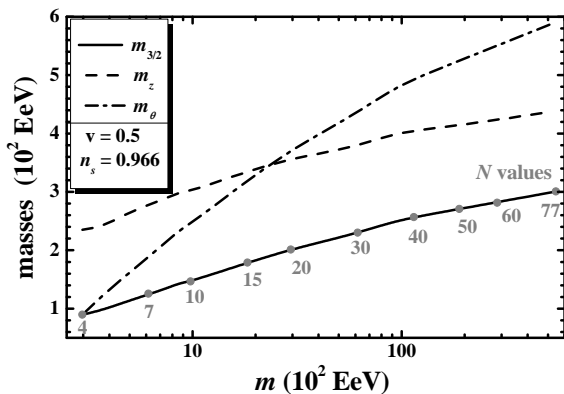


**FIG. 6:** Allowed values of  $m_{3/2}$ ,  $m_z$  and  $m_\theta$  (solid, dashed and dot-dashed line respectively) versus  $m$  for  $n_s \simeq 0.966$  and  $v = 0.5$ . Shown is also the variation of  $N$  in grey along the solid line.

– calculated by Eqs. (17), (16a) and (16b) respectively – as functions of  $m$  employing solid, dashed and dot-dashed lines correspondingly. Shown is also the variation of  $N$  along the solid line. In all, we have

$$2.3 \lesssim \frac{m_z}{100 \text{ EeV}} \lesssim 4.4 \quad \text{and} \quad 8.9 \lesssim \frac{m_\theta}{10 \text{ EeV}} \lesssim 59, \quad (48)$$

where the lower bound on  $m_\theta$  coincides with that on  $m_{3/2} = \tilde{m}$ . Note that the  $\widehat{\delta z}$  decay channel into  $\theta$ 's is kinematically blocked for  $N \gtrsim 20$ . We also find that for  $N \lesssim 10$ ,  $\Gamma_{\delta z} \simeq \Gamma_{3/2} + \Gamma_{\tilde{h}}$  whereas for larger  $N$ 's  $\Gamma_{\delta z} \simeq \Gamma_{\tilde{h}}$  and so Eq. (44a) yields  $T_{\text{rh}} \simeq (4 - 20) \text{ PeV}$  resulting to  $N_* \simeq (45.5 - 46.7)$ . The obtained  $a_s \simeq -(3.1 - 3.2) \cdot 10^{-3}$  might be detectable in future [30].

Throughout our investigation, we assumed that the slow-roll approximation offers a reliable description of IPI. This is a reasonable assumption since the observationally relevant part of IPI takes place for  $z_* < z_0$  – see e.g. inset of Fig. 2. However, we do not address in this letter the question of how  $z$  reaches  $z_0$ , that is, the problem of the initial conditions for inflation. Since  $V_1$  is extremely flat close to  $z_0$ , there is the danger that the system temporarily undergoes a period of the so-called ultra-slow-roll evolution [42–44], where the gradient of  $V_1$  may be neglected rather than the acceleration of  $z$  in the Klein-Gordon equation. However, this danger can be averted [43], if we assume that the  $z$  lies initially near  $z_0$  with a small enough kinetic energy density which is at most the one corresponding to the slow-roll phase,

$$\rho_K^{\text{max}} \simeq \epsilon(z_0) V_1(z_0) / 3. \quad (49a)$$

Under such a condition, the slow roll starts immediately and all our findings are perfectly valid. E.g., for the range of the parameters in Fig. 6, we find

$$1.4 \lesssim (\rho_K^{\text{max}})^{1/4} / 10^3 \text{ EeV} \lesssim 3.2, \quad (49b)$$

where the upper/lower bound corresponds to the respective  $N$  bounds in Fig. 6 and turn out to be two orders of magnitude less than  $V_1(z_0)^{1/4}$ . Moreover, as shown for similar models [44], we can always find suitable initial conditions in the phase space of the system so as slow-roll IPI to take place. Since  $\epsilon(z)$  in a such case is a smooth increasing function without spikes, no production of black holes [42, 43] occurs.

## VI. CONCLUSIONS

Taking advantage from the self-stabilized no-scale models of SUSY breaking, established in Ref. [1, 2], we proposed a variant which incorporates IPI – i.e., inflection-point inflation – realized by the sgoldstino. The inflationary model results to an adjustable  $n_s$ , a small  $r$  and a sizable  $a_s$  of the order of  $-10^{-3}$ . Linking our model to MSSM we showed that SUSY may be broken at a dS vacuum, providing the correct DE density parameter – at the cost of a fine-tuned parameter – and a SUSY mass scale  $\tilde{m} \sim 100 \text{ EeV}$  which is consistent with the Higgs boson mass measured at LHC. Needless to say, the stability of the electroweak vacuum up to the Planck scale is automatically assured within our framework.

It would be interesting to investigate if the intermediate-scale lightest neutralino with mass  $M_1$  in the interval  $T_{\text{rh}} < M_1 < T_{\text{max}}$  is a good cold dark matter candidate adapting the non-equilibrium production [45]. Here,  $T_{\text{max}}$  is the maximal temperature during reheating and may be as high as  $10^3 T_{\text{rh}}$  [45]. Also, baryogenesis via non-thermal leptogenesis [46] may be activated even without direct coupling of the sgoldstino to right-handed neutrinos. Our model, most probably, does not belong to the string swampland [47] but it is amenable to modifications [48] which may render it more friendly with the string ultraviolet completions.

**ACKNOWLEDGMENTS** I would like to thank Mar Bastero-Gil for an interesting discussion. This research work was supported by the Hellenic Foundation for Research and Innovation (H.F.R.I.) under the “First Call for H.F.R.I. Research Projects to support Faculty members and Researchers and the procurement of high-cost research equipment grant” (Project Number: 2251).

## REFERENCES

- [1] J. Ellis, B. Nagaraj, D.V. Nanopoulos and K.A. Olive, *J. High Energy Phys.* **11**, 110 (2018) [arXiv:1809.10114]; J. Ellis, B. Nagaraj, D.V. Nanopoulos, K.A. Olive and S. Verner, *J. High Energy Phys.* **10**, 161 (2019) [arXiv:1907.09123].
- [2] C. Pallis, *Eur. Phys. J. C* **83**, no. 4, 328 (2023) [arXiv:2211.05067].
- [3] E. Cremmer, S. Ferrara, C. Kounnas and D.V. Nanopoulos, *Phys. Lett. B* **133**, 61 (1983); J.R. Ellis, C. Kounnas and D.V. Nanopoulos, *Nucl. Phys.* **B241**, 406 (1984).

- [4] D.Z. Freedman and A. Van Proeyen, *Supergravity*. Cambridge University Press, 2012.
- [5] J. Ellis, D.V. Nanopoulos, K.A. Olive and S. Verner, *Phys. Rev. D* **100**, no. 2, 025009 (2019) [arXiv:1903.05267]; *J. Cosmol. Astropart. Phys.* **09**, 040 (2019) [arXiv:1906.10176]; *J. Cosmol. Astropart. Phys.* **08**, 037 (2020) [arXiv:2004.00643].
- [6] J. Ellis, M.A.G. Garcia, N. Nagata, D.V. Nanopoulos, K.A. Olive and S. Verner, *Int. J. Mod. Phys. D* **29**, 16, 2030011 (2020) [arXiv:2009.01709].
- [7] N. Aghanim *et al.* [Planck Collaboration], *Astron. Astrophys.* **641**, A6 (2020) [arXiv:1807.06209].
- [8] S. Kachru, R. Kallosh, A.D. Linde and S. P. Trivedi, *Phys. Rev. D* **68**, 046005 (2003) [hep-th/0301240]; S. Kachru *et al.*, *J. Cosmol. Astropart. Phys.* **10**, 013 (2003) [hep-th/0308055].
- [9] N. Cribiori, F. Farakos, M. Tournoy and A. Van Proeyen, *J. High Energy Phys.* **04**, 032 (2018) [arXiv:1712.08601]; I. Antoniadis, A. Chatrabhuti, H. Isono, and R. Knoops, *Eur. Phys. J. C* **78**, 718 (2018) [arXiv:1805.00852]; I. Antoniadis, Y. Chen and G.K. Leontaris, *Eur. Phys. J. C* **78**, 9, 766 (2018) [arXiv:1803.08941]; I. Antoniadis, Y. Chen and G.K. Leontaris, *J. High Energy Phys.* **01**, 149 (2020) [arXiv:1909.10525]; O. Guleryuz, arXiv:2207.10634.
- [10] G. Aad *et al.* (ATLAS Collaboration), *Phys. Rev. D* **90**, 052004 (2014); CMS Collaboration, Tech. Rep. CMS-PAS-HIG-14-009 (2014).
- [11] R. Kallosh and A. Linde, *Phys. Rev. D* **91**, 083528 (2015) [arXiv:1502.07733]; A. Linde, *J. Cosmol. Astropart. Phys.* **11**, 002 (2016) [arXiv:1608.00119].
- [12] Y. Aldabergenov and S.V. Ketov, *Phys. Lett. B* **761**, 115 (2016) [arXiv:1607.05366]; Y. Aldabergenov, A. Chatrabhuti and S.V. Ketov, *Eur. Phys. J. C* **79**, no. 8, 713 (2019) [arXiv:1907.10373].
- [13] M.C. Romão and S.F. King, *J. High Energy Phys.* **07**, 033 (2017) [arXiv:1703.08333]; S.F. King and E. Perdomo, *J. High Energy Phys.* **05**, 211 (2019) [arXiv:1903.08448].
- [14] S.V. Ketov and T. Terada, *J. High Energy Phys.* **12**, 062 (2014) [arXiv:1408.6524]; A. Linde, D. Roest and M. Scalisi, *J. Cosmol. Astropart. Phys.* **03**, 017 (2015) [arXiv:1412.2790].
- [15] K. Harigaya and K. Schmitz, *Phys. Lett. B* **773**, 320 (2017) [arXiv:1707.03646]; V. Domcke and K. Schmitz, *Phys. Rev. D* **97**, no. 11, 115025 (2018) [arXiv:1712.08121].
- [16] S. Ferrara and D. Roest, *J. Cosmol. Astropart. Phys.* **10**, 038 (2016) [arXiv:1608.03709].
- [17] A. Achucarro, S. Mooij, P. Ortiz and M. Postma, *J. Cosmol. Astropart. Phys.* **08**, [ (2012) arXiv:1203.1907].
- [18] I. Antoniadis, A. Chatrabhuti, H. Isono and R. Knoops, *Eur. Phys. J. C* **77**, no. 11, 724 (2017) [arXiv:1706.04133].
- [19] Y. Aldabergenov, A. Chatrabhuti and H. Isono, *Eur. Phys. J. C* **81**, no. 2, 166 (2021) [arXiv:2009.02203].
- [20] T.J. Gao and Z.K. Guo, *Phys. Rev. D* **91**, 123502 (2015) [arXiv:1503.05643].
- [21] C. Pallis, *Eur. Phys. J. C* **82**, no. 5, 444 (2022) [arXiv:2204.01047].
- [22] J. Martin, C. Ringeval and V. Vennin, *Phys. Dark Univ.* **5**, 75 (2014) [arXiv:1303.3787]; J. Martin, C. Ringeval R. Trotta and V. Vennin, *J. Cosmol. Astropart. Phys.* **03**, 039 (2014) [arXiv:1312.3529].
- [23] R. Allahverdi, K. Enqvist, J. Garcia-Bellido and A. Mazumdar, *Phys. Rev. Lett.* **97**, 191304 (2006) [hep-ph/0605035]; K. Enqvist, A. Mazumdar and P. Stephens, *J. Cosmol. Astropart. Phys.* **06**, 020 (2010) [arXiv:1004.3724].
- [24] J.C. Bueno Sanchez, K. Dimopoulos and D.H. Lyth, *J. Cosmol. Astropart. Phys.* **01**, 015 (2007) [hep-ph/0608299].
- [25] N. Itzhaki and E. D. Kovetz, *J. High Energy Phys.* **10**, 054 (2007) [arXiv:0708.2798]; A.D. Linde and A. Westphal, *J. Cosmol. Astropart. Phys.* **03**, 005 (2008) [arXiv:0712.1610]; M. Badziak and M. Olechowski, *J. Cosmol. Astropart. Phys.* **02**, 010 (2009) [arXiv:0810.4251].
- [26] S.-M. Choi and H.M. Lee, *Eur. Phys. J. C* **76** 303, no. 6 (2016) [arXiv:1601.05979]; K. Dimopoulos, C. Owen and A. Racioppi, *Astropart. Phys.* **103**, 16 (2018) [arXiv:1706.09735]; N. Okada, S. Okada and D. Raut, *Phys. Rev. D* **95**, no.5, 055030 (2017) [arXiv:1702.02938].
- [27] M. Drees and Y. Xu, *J. Cosmol. Astropart. Phys.* **09**, 012 (2021) [arXiv:2104.03977].
- [28] Y. Akrami *et al.* [Planck Collaboration], *Astron. Astrophys.* **641**, A10 (2020) [arXiv:1807.06211].
- [29] P.A.R. Ade *et al.*, *Phys. Rev. Lett.* **121**, 221301 (2018) [arXiv:1810.05216].
- [30] J.B. Muñoz *et al.*, *J. Cosmol. Astropart. Phys.* **05**, 032 (2017) [arXiv:1611.05883].
- [31] L.J. Hall and Y. Nomura, *J. High Energy Phys.* **03**, 076 (2010) [arXiv:0910.2235]; L.E. Ibáñez and I. Valenzuela, *J. High Energy Phys.* **05**, 064 (2013) [arXiv:1301.5167].
- [32] E. Bagnaschi, G.F. Giudice, P. Slavich and A. Strumia, *J. High Energy Phys.* **09**, 092 (2014) [arXiv:1407.4081].
- [33] S.P. Martin, *Adv. Ser. Direct. High Energy Phys.* **18**, 1 (1998) [hep-ph/9709356].
- [34] A. Brignole, L.E. Ibáñez and C. Muñoz, *Adv. Ser. Direct. High Energy Phys.* **18**, 125 (1998) [hep-ph/9707209].
- [35] C. Pallis, *Nucl. Phys. B* **751**, 129 (2006) [hep-ph/0510234]; J. Ellis *et al.*, *Phys. Rev. D* **105**, no.4, 043504 (2022) [arXiv:2112.04466].
- [36] M. Endo, F. Takahashi and T.T. Yanagida, *Phys. Rev. D* **76**, 083509 (2007) [arXiv:0706.0986].
- [37] J. Ellis, M. Garcia, D. Nanopoulos and K. Olive, *J. Cosmol. Astropart. Phys.* **10**, 003 (2015) [arXiv:1503.08867].
- [38] Y. Aldabergenov, I. Antoniadis, A. Chatrabhuti and H. Isono, *Eur. Phys. J. C* **81**, no. 12, 1078 (2021) [arXiv:2110.01347].
- [39] K.J. Bae, H. Baer, V. Barger and R.W. Deal, *J. High Energy Phys.* **02**, 138 (2022) [arXiv:2201.06633].
- [40] G. 't Hooft, *NATO Sci. Ser. B* **59**, 135 (1980).
- [41] G. Lazarides and C. Pallis, *J. High Energy Phys.* **11**, 114 (2015) [arXiv:1508.06682].
- [42] C. Germani and T. Prokopec, *Phys. Dark Univ.* **18**, 6 (2017) [arXiv:1706.04226]; J. Garcia-Bellido and E. Ruiz Morales, *Phys. Dark Univ.* **18**, 47 (2017) [arXiv:1702.03901].
- [43] K. Dimopoulos, *Phys. Lett. B* **775**, 262 (2017) [arXiv:1707.05644].
- [44] C. Pattison, V. Vennin, H. Assadullahi and D. Wands, *J. Cosmol. Astropart. Phys.* **08**, 048 (2018) [arXiv:1806.09553]; Y. Bai and D. Stolarski, *J. Cosmol. Astropart. Phys.* **03**, 091 (2021) [arXiv:2008.09639].
- [45] D.J.H. Chung, E.W. Kolb and A. Riotto, *Phys. Rev. Lett.* **81**, 4048 (1998) [hep-ph/9805473]; D.J.H. Chung, E.W. Kolb and A. Riotto, *Phys. Rev. D* **59**, 023501 (1998) [hep-ph/9802238].
- [46] G. Lazarides and Q. Shafi, *Phys. Lett. B* **258**, 305 (1991); G. Lazarides, hep-ph/9905450; K. Kumekawa, T. Moroi, and T. Yanagida, *Prog. Theor. Phys.* **92**, 437 (1994) [hep-ph/9405337].
- [47] C. Vafa, hep-th/0509212; S.K. Garg and C. Krishnan, *J. High Energy Phys.* **11**, 075 (2019) [arXiv:1807.05193]; H. Ooguri, E. Palti, G. Shiu and C. Vafa, *Phys. Lett. B* **788**, 180 (2019) [arXiv:1810.05506].
- [48] I.M. Rasulian, M. Torabian and L. Velasco-Sevilla, *Phys. Rev. D* **104**, no. 4, 044028 (2021) [arXiv:2105.14501].